

Skin Debris on the Face of the Turin Shroud: A SEM-EDX Analysis

G rard Lucotte

Institute of Molecular Anthropology, Paris, France

Email: luccotte@hotmail.com

Received 4 March 2016; accepted 24 April 2016; published 27 April 2016

Copyright   2016 by author and Scientific Research Publishing Inc.

This work is licensed under the Creative Commons Attribution International License (CC BY).

<http://creativecommons.org/licenses/by/4.0/>



Open Access

Abstract

Aim: We have studied the only found three skin debris (P1, P2 and P3) deposited on the Face area of our sample of the Turin Shroud. **Methods:** P1, P2 and P3 were explored by optical microscopy, by SEM and by EDX analysis. **Results:** All P1, P2 and P3 are true skin debris, as observed in optic and electronic microscopy; their elementary compositions show organic matter, plus a sulphur peak that corresponds to keratin. P1, P2 and P3 are constituted of layers of corneocytes; in P3, which is certainly a human skin debris, we can observe both the epidermis and some residual dermis.

Keywords

Turin Shroud, Face Area, Skin Debris, Optical Microscopy and SEM, EDX Analysis

1. Introduction

The Turin Shroud (TS) is a well-known object in which a body image is imprinted (Marion & Lucotte, 2006). In 1978 and in 1988, Giovanni Riggi di Numana took some samples and dusts (Riggi di Numana, 1988) of the TS, at areas corresponding to Hands, Face (a 1978 sample taken on the Face area was deposited by him on a special sticky-tape), Feet, Buttocks and the ¹⁴C area. We had access to this sticky-tape, cutted up in a triangular form, and realised on it preliminary investigations (Lucotte, 2012) concerning mineral particles.

I have recently published three other studies on the triangle: the first one (Lucotte, 2015a) concerned linen (and other textile) fibers. The second (Lucotte, 2015b) concerned pollens (and spores); and the third (Lucotte, 2015c) red blood cells.

Desquamated epithelial cells—named as “skin debris” (SD)—were previously studied by SEM-EDX (Varetto, 1990; DeGaetano *et al.*, 1992), specially in a forensic science perspective (Burnett, 1995). In the present study, we describe in details some SD located on the triangle surface.

2. Materials and Methods

The material (Lucotte, 2012) is a small (1.36 mm high, 614 μm wide) sticky-tape triangle (Figure 1,

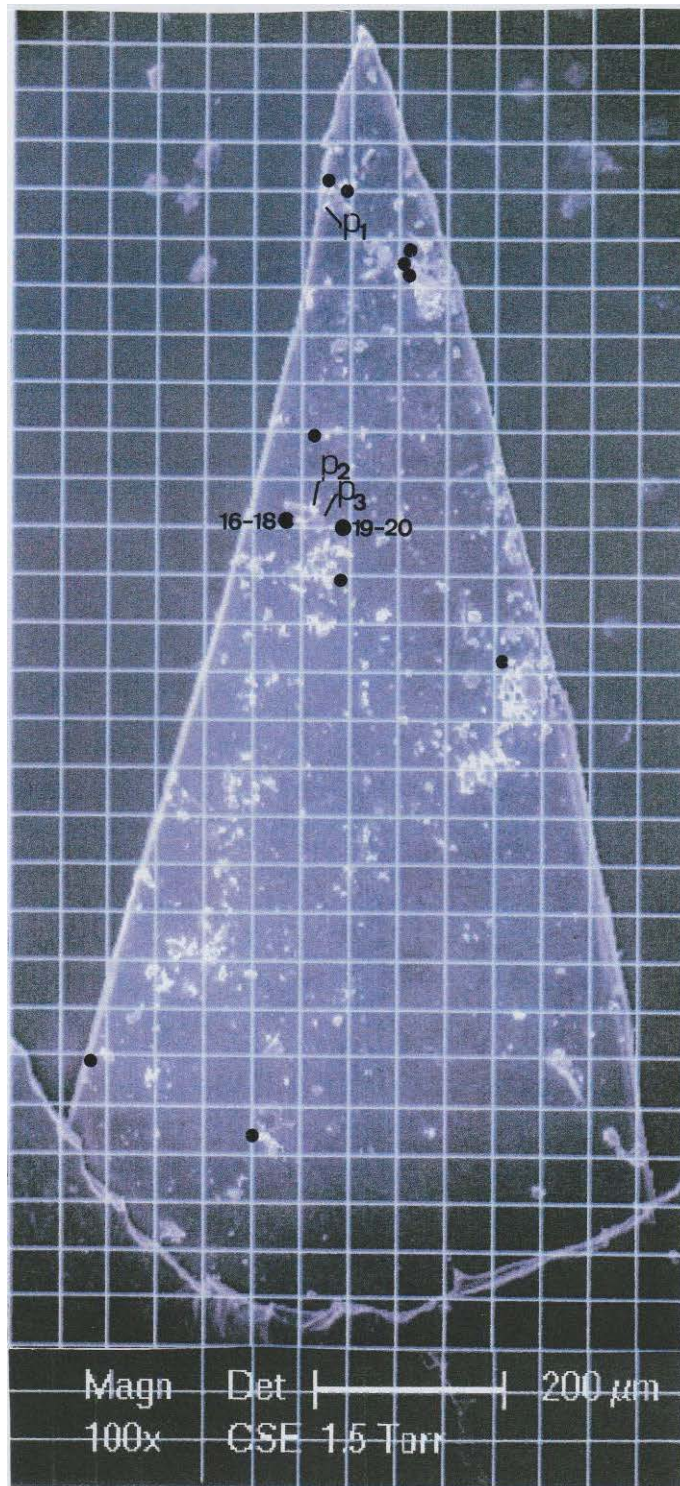


Figure 1. Locations of P1, P2 and P3 particles on the surface of the triangle (magnification factor: 100x). The black dots at each side of P3 indicate the hematy-group 16-18 and the hematy-group 19-20, respectively. Other smaller black dots indicates other hematies or hematy-groups on the surface of the triangle (Lucotte, 2015c).

the end of this article) at the surface of which the portions of fibers, pollen grains, red-blood cells and some plaques of organic matter were deposited.

More than 2500 particles, greater than $1\ \mu\text{m} = 1\ \mu$, can be observed at the surface of the triangle. All of them were studied by optical microscopy, SEM (Scanning Electronic Microscopy) and EDX (Energy Dispersive X-ray) analysis. For practical reasons, the surface of the triangle was subdivided into 19 sub-samples areas (areas A to S), the area E being subdivided in five sub-areas E.a to E.e), containing almost all the particles observed. The positions of each particle sticking to the triangle surface were located in a double system of coordinates (in 186 adjacent squares of $50 \times 50\ \mu$ of the total surface).

Cell debris of the samples were observed, without any preparation, on the adherent part of the surface of the triangle. The observations were conducted by SEM, using a Philips XL30 instrument (environmental version); GSE (Gaseous Secondary Electrons) and BSE (Back Scattering Electrons) procedures were used, the last one to detect heavy material. Elemental analyses for each skin debris were realised by X-ray microfluorescence (XRMF), this SEM microscope being equipped with a Bruker AXS energy dispersive X-ray (EDX); the system of analysis is PGT (Spirit Model, of Princeton Gamma Technology).

Our SEM studies were completed by the optical observations of cell debris numbers 1, 2 and 3 (using a photomicroscope Zeiss, model III, 1972) and by their study in cross-polarized light (with the petrographic version of this microscope).

3. Results

As an example, **Figure 2** shows the aspect (in SEM) and the EDX spectrum of a little layer of skin corneous

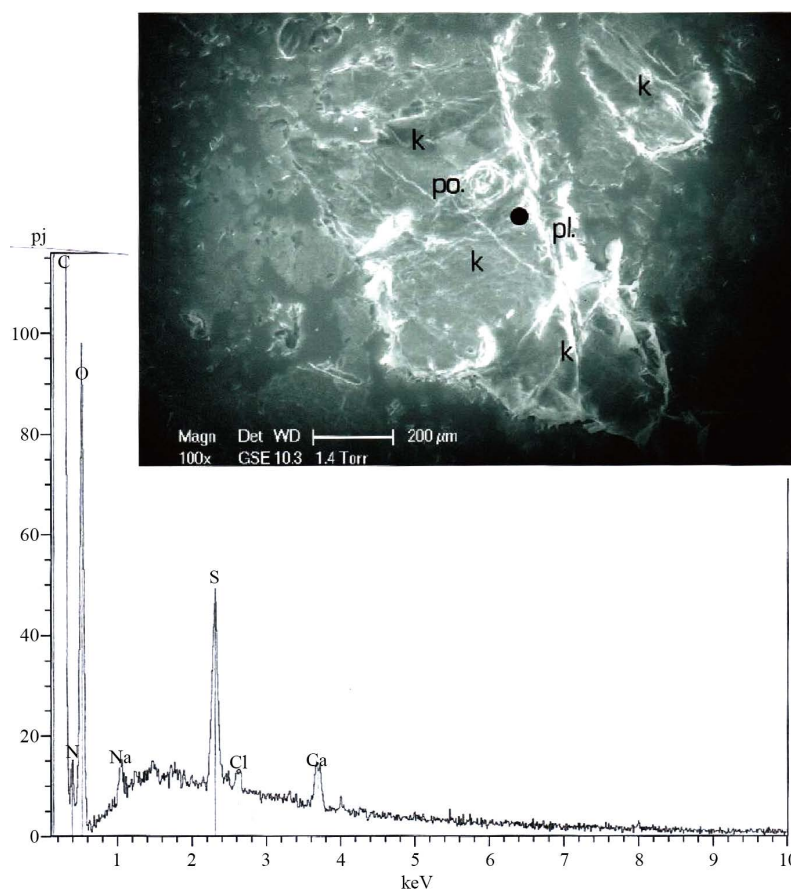


Figure 2. Above: SEM photography (100×) of a fragment of corneous layers taken on the face of a living man; k indicates several surface areas of adjacent corneocytes (po: pore; pl: pleat). Below: EDX spectrum resulting from elementary analysis at the black point indicated on the photography. Peaks correspond to C: carbon, N: nitrogen, Na: sodium, S: sulphur, Cl: chlorine, Ca: calcium.

cells taken on the face of a 30-years old living man. We see on the SEM photography several large superposed corneous cells. EDX analysis of one of them shows an elementary composition rich in organic matter (carbon, oxygen and nitrogen) and a secondary peak of sulphur (keratin); also in the spectrum are little peaks of chlorine and sodium (ClNa: salt of the sweat) and of calcium (residual minerals deposited on the skin surface).

We have found only three SD on the triangle:

The a37 particle, located in the A area

This particle is the first SD (designated as P1) observed on the surface of the triangle. The SEM photography of **Figure 3** shows the mean characteristics of the visible part of P1: it is a little surface (of about 10 μ of length) of skin, with two layers at least, the upper one being rough in aspect.

The P1 spectrum shows peaks corresponding to the constitutive elements (carbon, oxygen and sulphur) of the skin and of the sweat (chlorine and sodium). But the major secondary peaks of the spectrum are those of silicium and calcium; magnesium and aluminium (and probably also potassium and iron) are elements associated to silicium, to constitute a clay mineral of the montmorillonite-illite type (Lucotte, 2012).

Figure 4 gives another P1 spectrum; here elements are quantified, to distinguish between those being skin specific to those concerning mineral deposits. The calcium component represents about 23.4% of all elements (carbon and oxygen expected); the silicate component (comprising silicium, plus aluminium and magnesium) represents about 41% of the total. So, this P1 SD fragment is importantly covered by mineral clay deposits.

It seems that there are remarkable similarities (**Figure 5**), both in aspect and in composition, between P1 and a SD fragment of some part of my own finger skin (a clean SD, detached at the top of one of my finger). We suggest that P1 is a SD finger fragment originating from some of the many persons that have touched, in the past

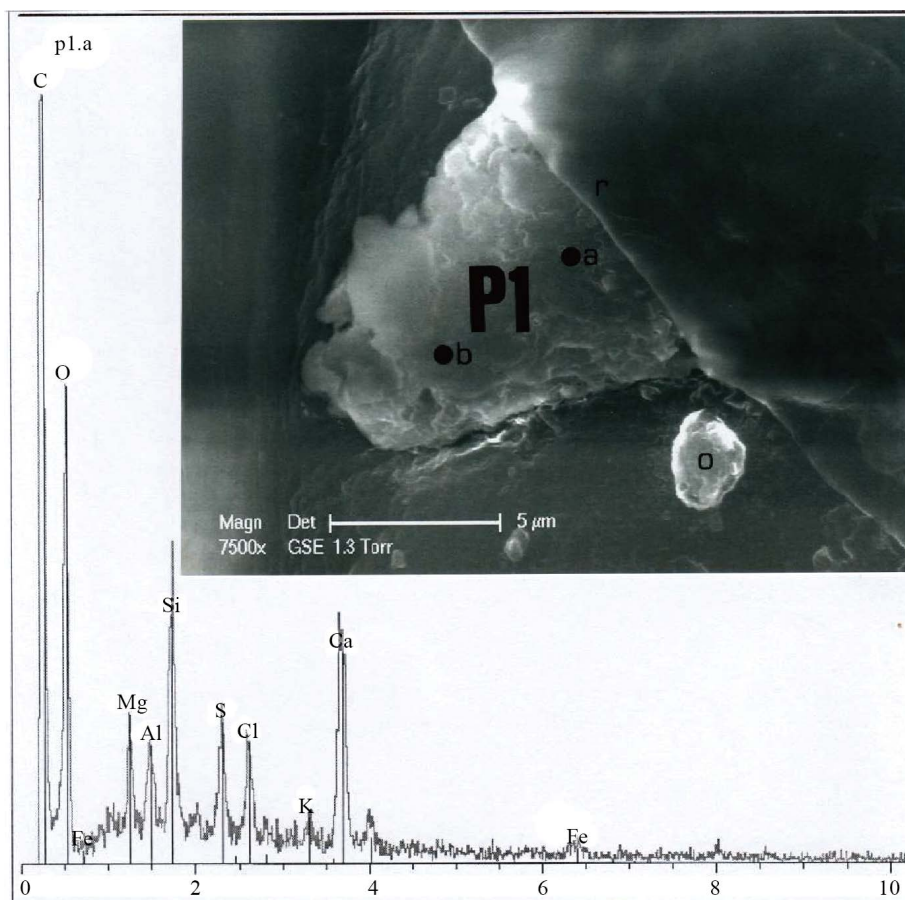


Figure 3. Above: SEM photography (x7500) of P1. The adjacent particle 0 (a38) is a micro-ball of organic matter; the right part of P1 is completely covered by a thin film of plastic matter (r) of PVC (vinyl polychlorure). Below: EDX spectrum at p1.a. Mineral peaks correspond to Mg: magnesium, Al: aluminium, Si: silicium and Ca: calcium; there are traces of K: potassium, and Fe: iron.

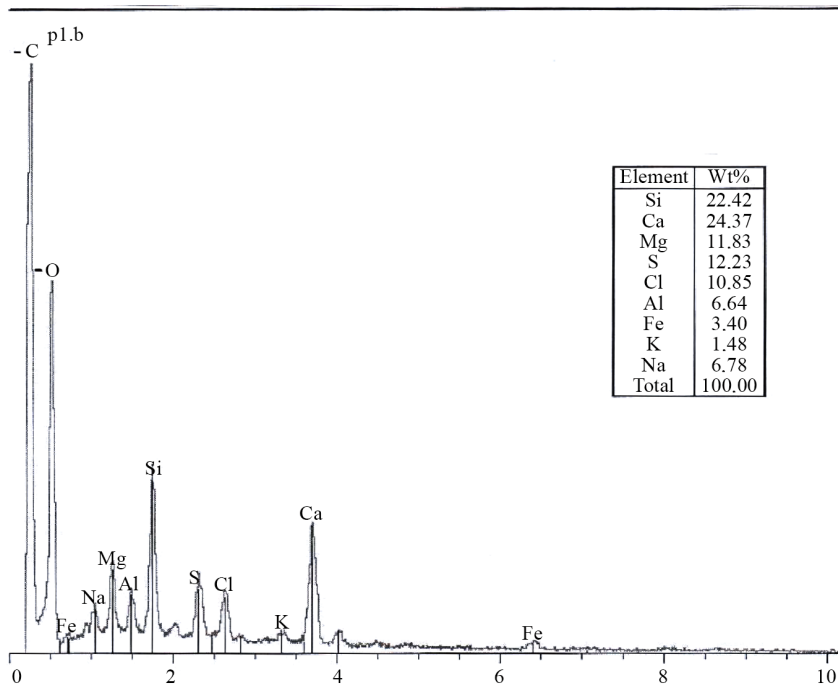


Figure 4. EDX spectrum at p1.b. The table summarizes the proportions of some elements.

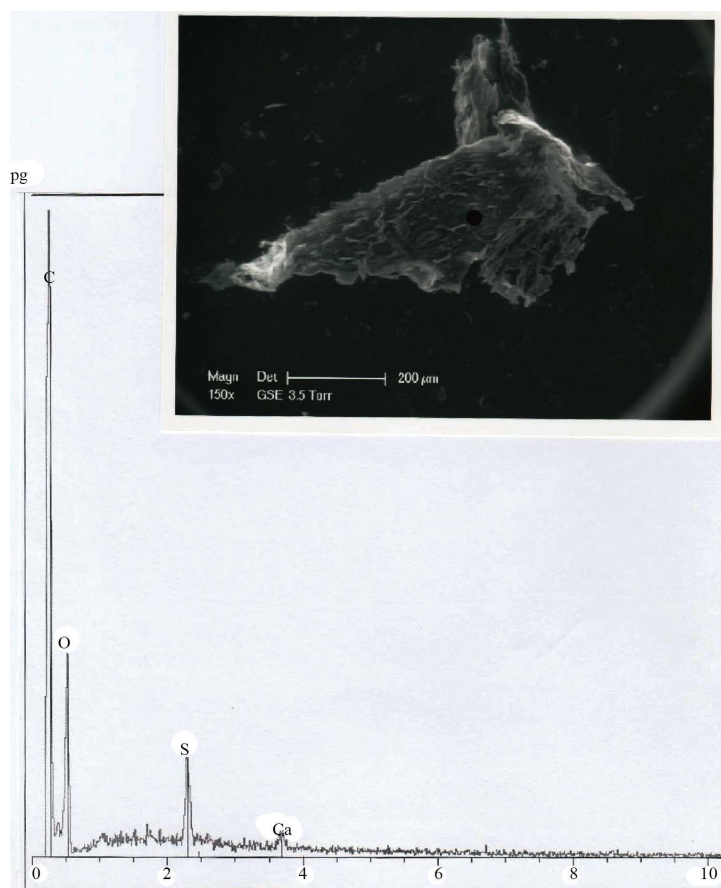


Figure 5. Above: SEM photography (150x) of a skin debris of top-finger. Below: spectrum at the black point indicated.

(because it is now covered by mineral deposits, accumulated since the time), the TS; but further studies on P1 are problematic, because its most important surface part is covered by a thin plastic layer (**Figure 3**), impermeable to electrons.

The e2 particle, located in the E area (in sub-area E.a)

This particle is the second SD (designated as P2) observed on the triangle. The two SEM photographs of **Figure 6** show the main characteristics of P2: it corresponds to a relatively large surface (maximal length of about $17\ \mu$) of an ovaloïd skin fragment. The right upper border of P2 had some depth, with at least four layers.

The P2 surface is also rough. The below photography of **Figure 6** (taken in BSE) indicates that the P2 surface is entirely covered with a relatively heavy material.

Figure 7 gives the P2 spectrum. This SD is mainly composed of organic matter (carbon and oxygen), plus

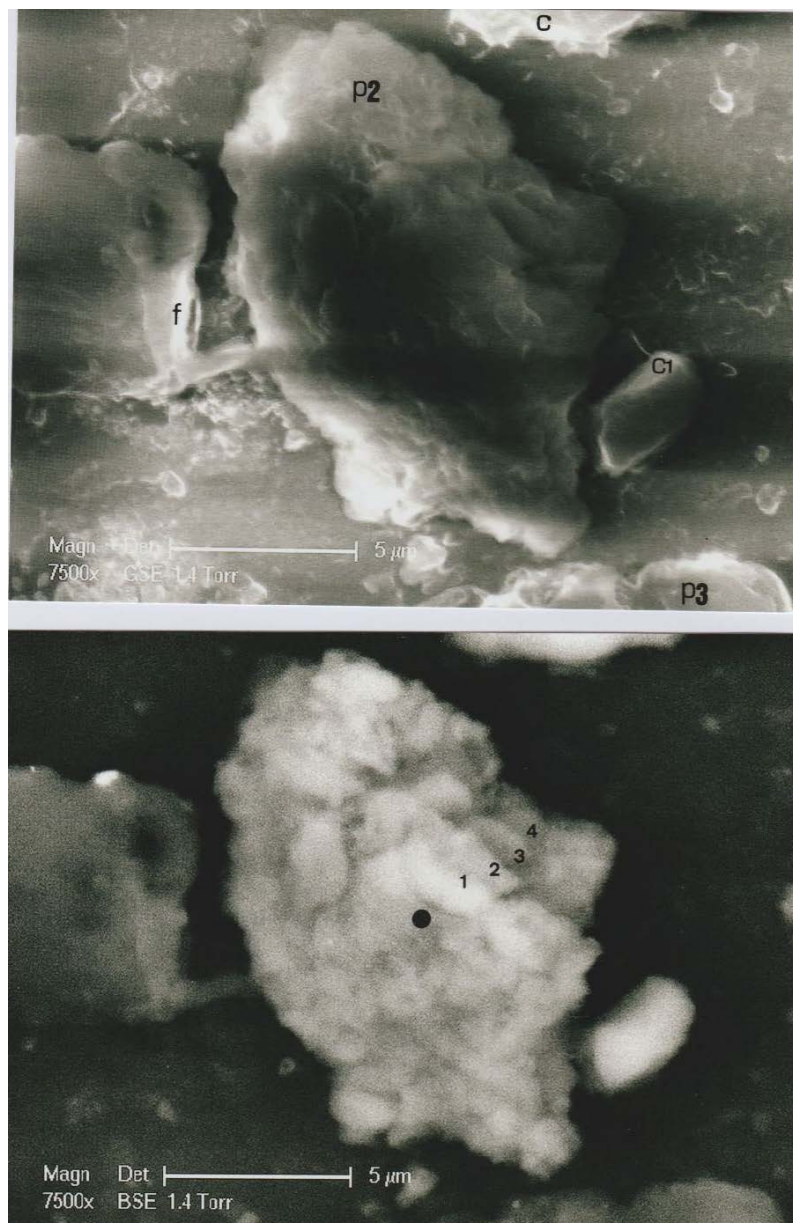


Figure 6. Above: SEM photography (7500 \times) of P2, in GSE. The adjacent particle f (e1) is a byssus micro-tubule; adjacent particle c (e3) is a calcium carbonate, and particle c1 (e4) is a calcium carbonate cristal of the aragonite type. Below is the upper part of P3. Below: the same (7500 \times) SEM photography of P2, but in BSE (1, 2, 3 and 4 indicate the successive layers of the thickness of the P2 particle); the black point is the micro-target where elementary analysis (**Figure 7**) was realised.

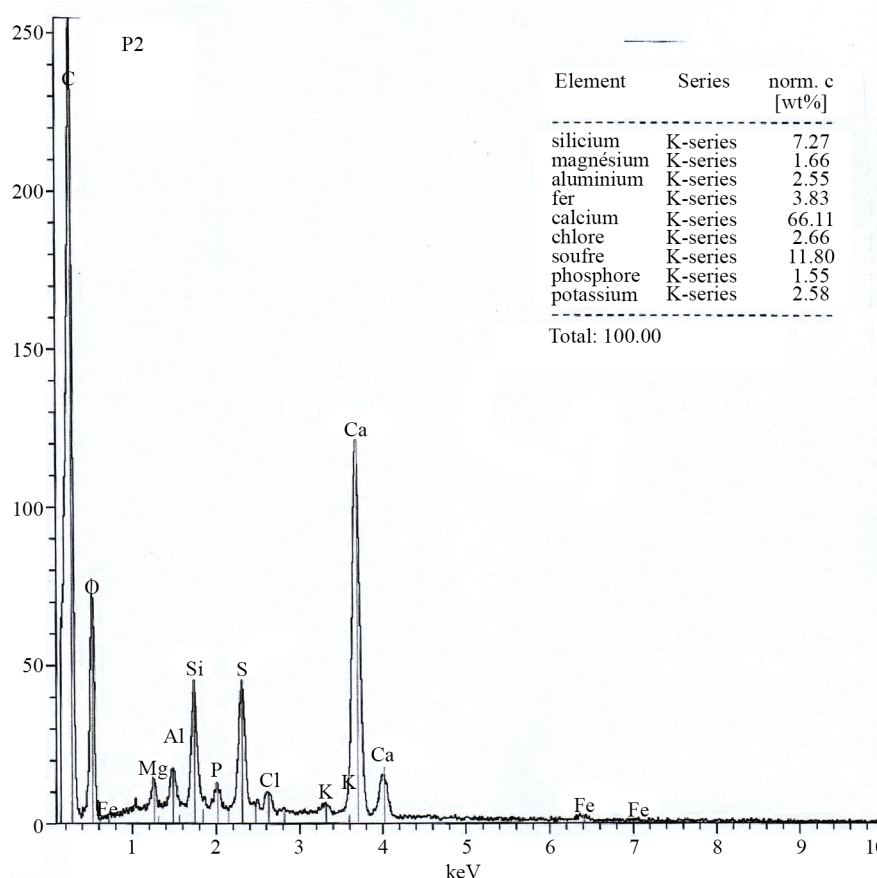


Figure 7. EDX spectrum of P2. The table summarizes the proportions of some elements.

sulphur (keratin); there are some traces of chlorine (and Na). But the calcium peak is very elevated, and the silicium peak is at the same level to that of sulphur. Quantification shows that—among the non-carbon and oxygen elements—the silicate component (silicium, aluminium and magnesium) represents only about 14.2% of the total, while the calcium component is at more than 66%. We conclude that the surface of the P2 skin fragment is mainly covered by a calcium carbonate deposit.

The e6 particle, located also in the Ea sub-area

This particle is the third SD observed on the triangle, and is designated as P3. The SEM photography of **Figure 8** shows its main characteristics: it corresponds to a large surface (maximal length of about 35 μ) of an elongated skin fragment. We can see, at the right upper part of the fragment, that it had some depth (because at least three layers are visible). The P2 lower part is adjacent to the upper part of P3 (**Figure 6**).

The P3 surface is sleek, with some micro-spines (**Figure 8** and **Figure 11**). We can distinguish on its surface some linear little reliefs that could correspond to cell limits of the keratinocytes.

The spectrum below the photography of **Figure 8** shows the elementary composition of P3 in its center. The predominant peaks (carbon and oxygen) are those of the organic matter, and there is a little peak of sulphur. Among the little peaks the chlorine peak is the most elevated, and there are some traces of sodium; there are also little peaks of calcium, and of silicium-aluminium-magnesium.

Both versions (in GSE and BSE) of the whole P3 particle are shown on **Figure 9** photographs. The retro-dif-fused view shows that almost all of the border of the upper-half P3 surface is covered by a thin layer of some matter, which is richer in heavy elements than the rest of the uncovered P3 surface.

Elementary analysis were realised both for a covered and an uncovered P3 surfaces (spectrums at the black points a and b on the photography of **Figure 10**, respectively). The spectrum corresponding to the black point a (an uncovered surface) is identical to that shown in **Figure 8**.

But the spectrum corresponding to the black point b (the most intensively covered surface portion) is distinct,

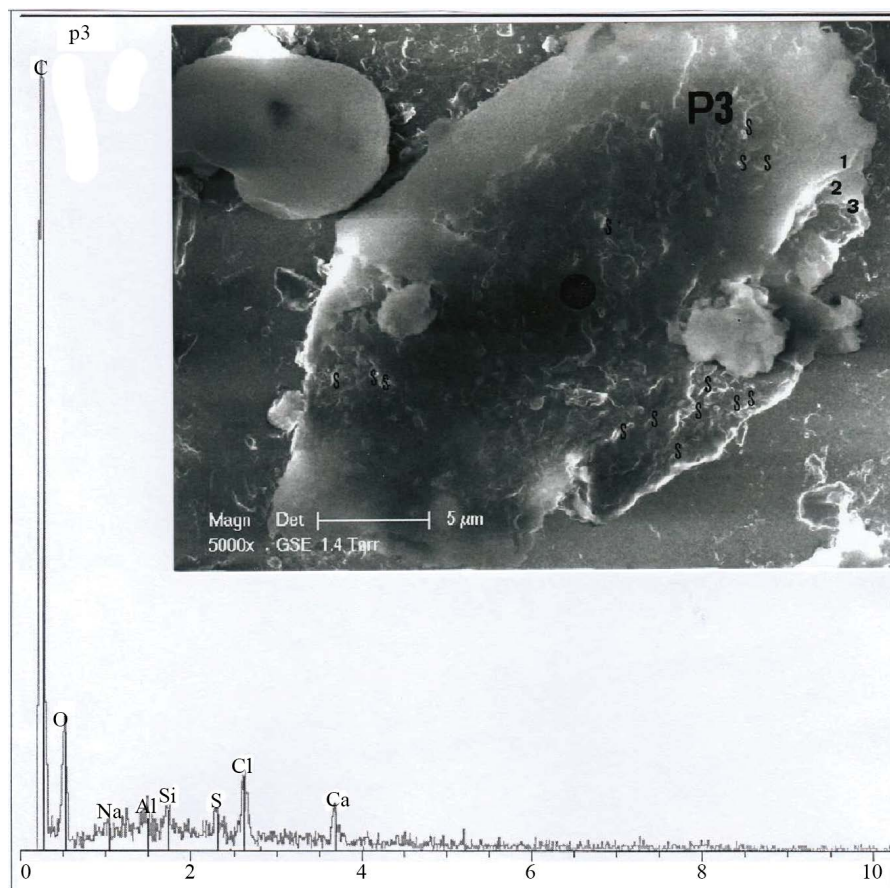


Figure 8. Above: SEM photography (5000 \times) of P3 (1, 2 and 3 indicate three layers; S: micro-spines). Black point in the center of P3 is the location where elementary analysis was realised. Below: spectrum at the black point.

for the little peaks upper spectrum of **Figure 10**), of these two last spectrums by two singularities: 1) A sodium peak appears; in that composition, sodium is not necessary linked to chlorine. 2) A nitrogen peak appears also; this relatively important level of nitrogen had probably something to do with a local “putrefaction process” of the P3 surface at this point.

The SEM photograph of **Figure 11** shows the enlarged ($\times 10,000$) square of the P3 area showed on **Figure 10** photograph. That permits to compare the smooth surface of the border of organic matter to that, delicately patterned and spinned, of the keratinocytes.

Study of the P1, P2 and P3 particles by optical microscopy

Figure 12 photographs concern optical views (in polarized light) of the A and E areas of the triangle, where particles P1, P2 and P3 are located. In **Figure 12**, photograph the entire P1 surface is shown; but is mostly covered (**Figure 13**) by a PVC plastic film, so not suitable to SEM-EDX analysis; the uncovered P1 surface can be distinguished on the photography, at a zone neighbouring the p38 particle (but this uncovered P1 surface is also partially masked by the triangle left border portion). The P1 particle of SD, yellow-grey in colour, does not show any birefringency when illuminated in polarized light.

Figure 12 photography shows that in its center the P2 and P3 particles are clearly identified by their shapes and sizes. The P2 surface shows birefringency (because of its elevated charge in calcium carbonate) when illuminated in polarized light, but that is not the case for the P3 surface, which had a relatively low calcium carbonate content. At each side of the P3 particle of SD can be distinguished the two h1 and h2 groups of red blood cells (Lucotte, 2015c); other adjacent P3 particles are not visible on the photography, because of masks (particles deposited at the surface, on the other side of the sticky-tape of the triangle).

The location of the P2 particle of the photography of **Figure 12**—determined by its position at the upper P3 border, and by its distance far from the right part of the e1 filament—is different to that shown in the SEM pho-

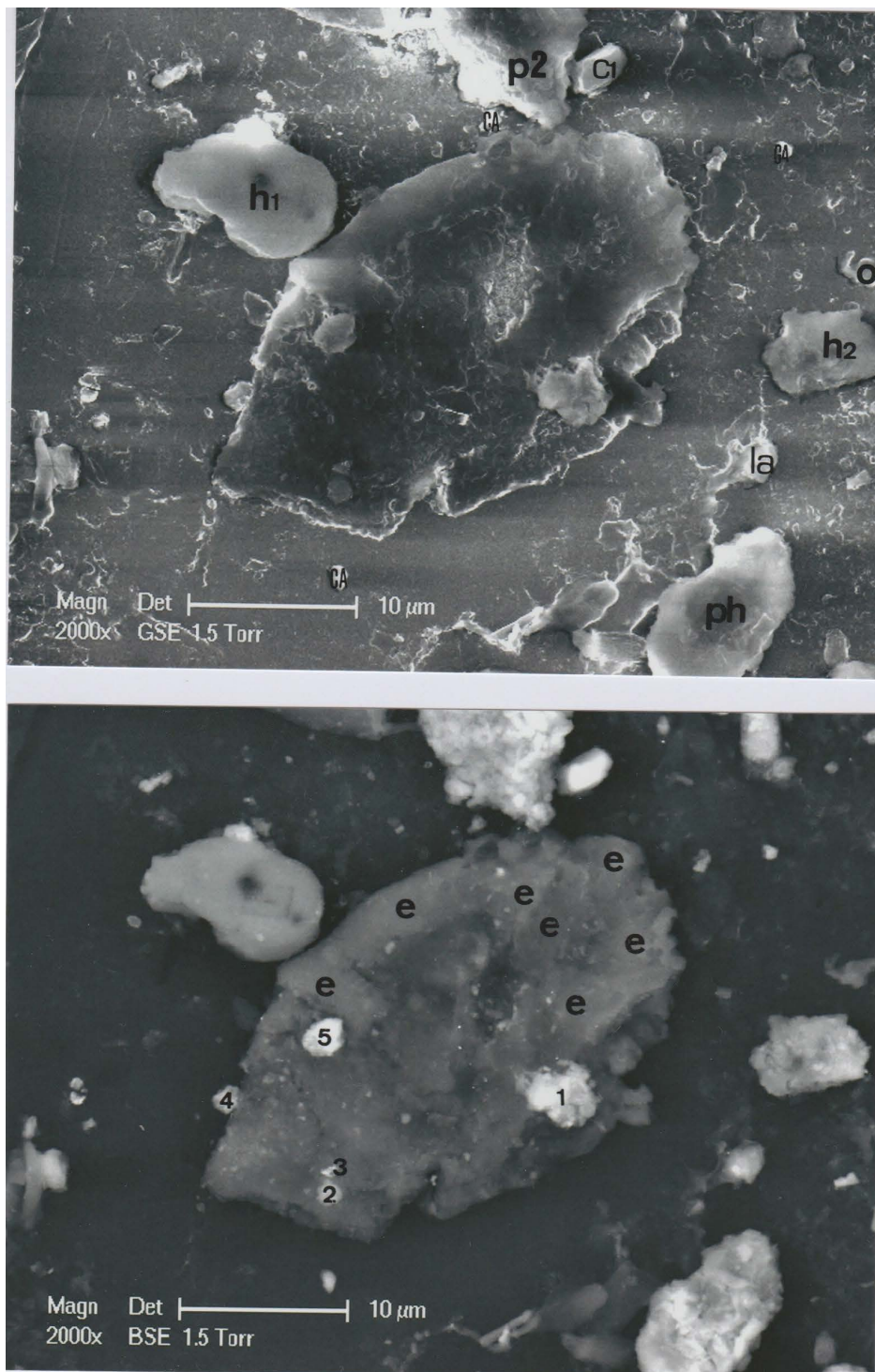


Figure 9. Above : SEM photography (2000×) of P3, in GSE. The lower P2 extremity is in contact to the upper P3 part. Adjacent particles to P3 are h1 (e5) and h2 (e 22), two red blood cells (piled up discocytes for h1 and two crenocytes for h2). Other main particles adjacent to P3 are: O (e23), constituted of organic matter; la (e21), a lapis-lazuli particle; ph (e7), a phosphorite iron-rich particle. CA are three calcite particles. Below: the same (2000×) SEM photography of P3, but in BSE. All the upper-half of P3 is covered by some matter (e), white in electrons. Sub-particles located in the lower half surface (corresponding to minerals and metals deposited on the inferior P3 part surface) of P3 are: 1, two lapis-lazuli sub-particles; 2, a calcite sub-particle; 3, a metallic sub-particle of a silver/copper alloy; 4, a clay of the chlorite type; 5, a mineral sub-particle of calcium carbonate.

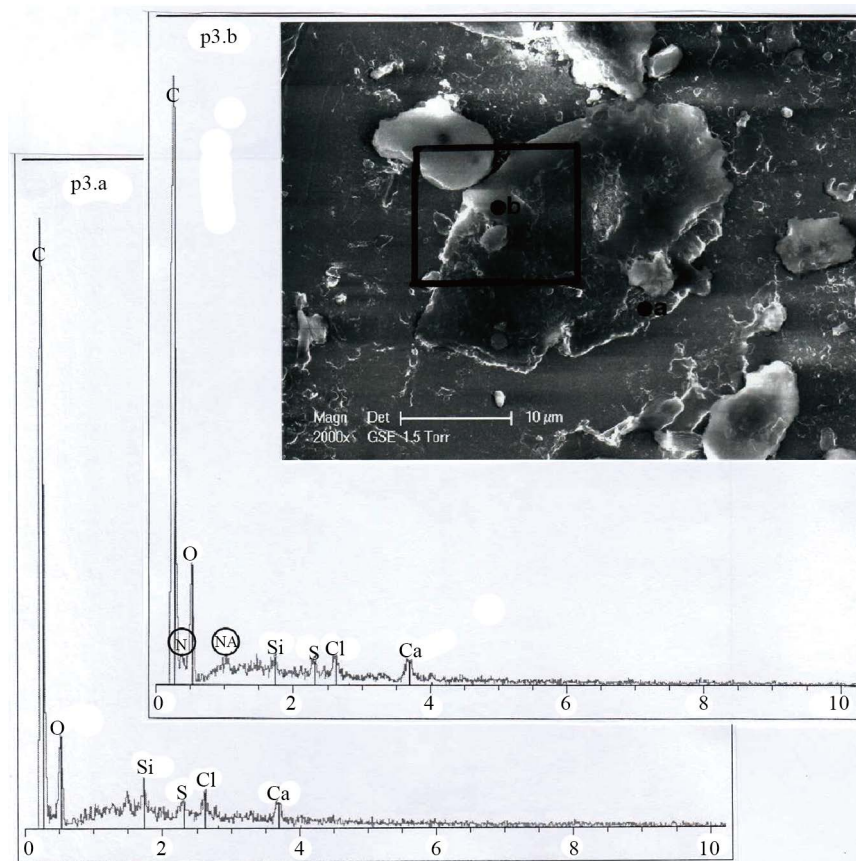


Figure 10. Above: the same SEM photography (2000×) of P3 that shown in the above **Figure 9** photography, where black points a and b are indicated. The P3 region in the square is enlarged on **Figure 11**. Below: spectrums at the black points a and b (nitrogen and sodium peaks are circled on the p3b spectrum).

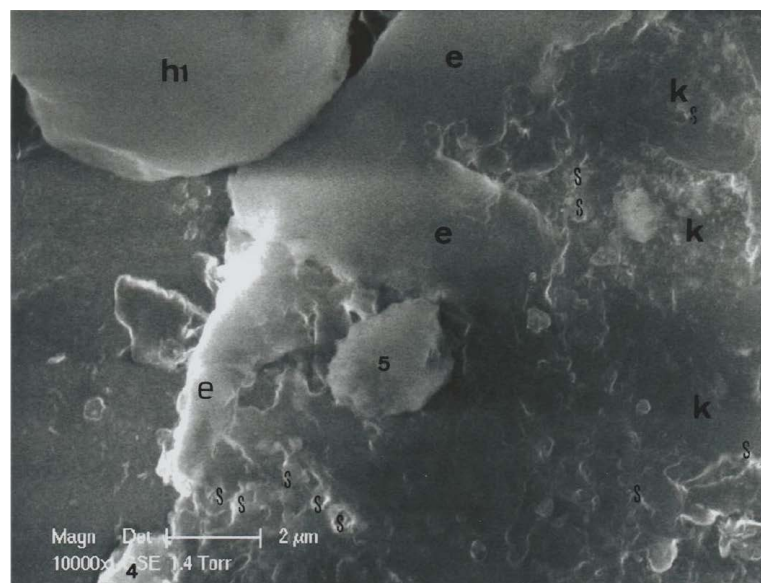


Figure 11. A SEM photography (10,000×) showing an enlarged view of the P3 region located in the square of **Figure 10**. The three e parts concern locations where white matter is denser; h1 is the e5 particle, and 4 and 5 are the sub-particles 4 and 5 of lower **Figure 9** photography. The three k areas show details on the keratinocytes surfaces (with micro-spines: S), uncovered by the e matter.

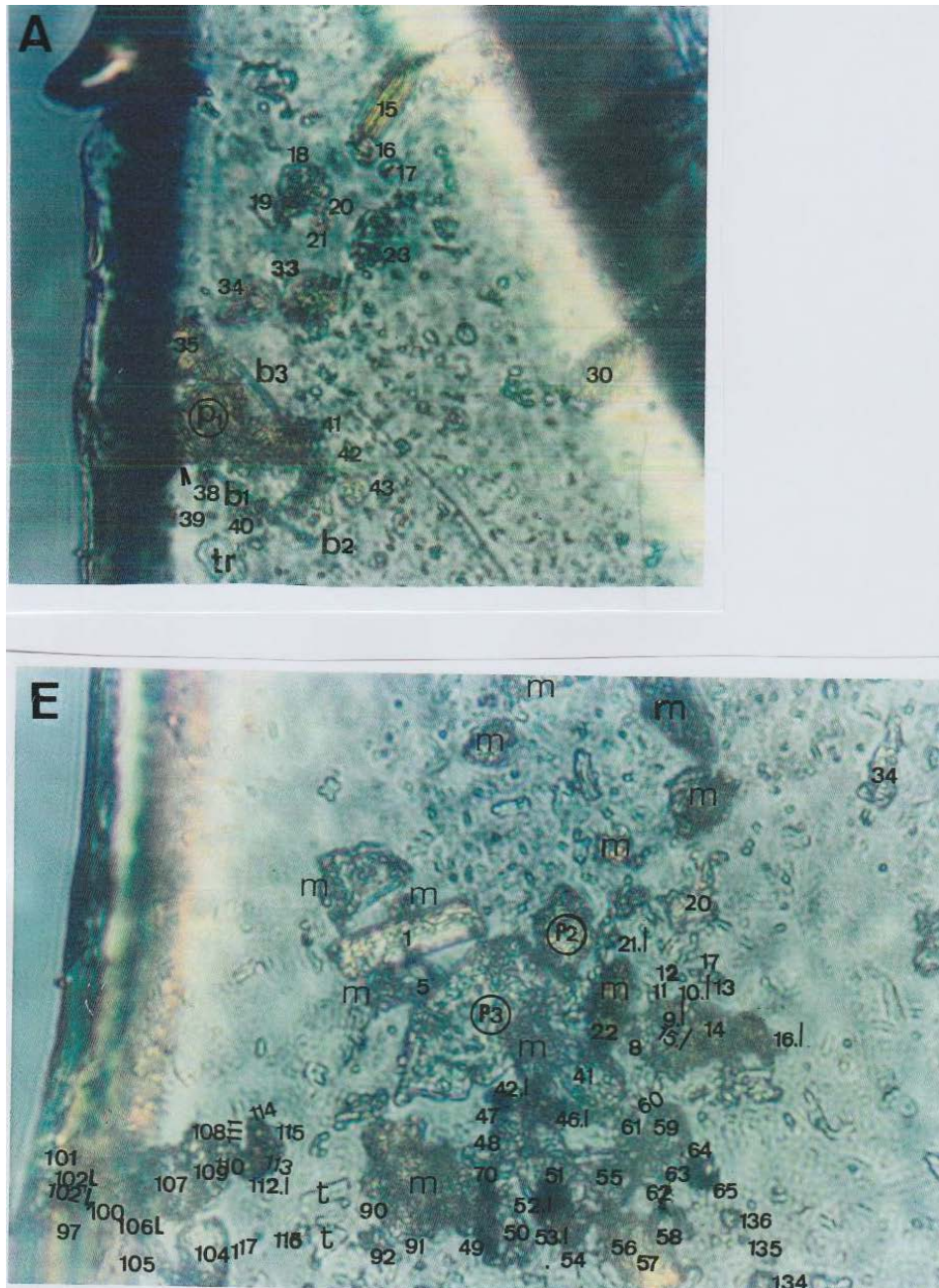


Figure 12. Optical microscopy views (1000 \times) of areas A and E. Above: a partial A area view (in polarized light) of the triangle, showing the P1 (encircled) particle; b1, b2 and b3 indicate the three PVC plastic borders (blue-green in colour). Number 38 indicates the a38 particle; the arrow point, located near the a38 particle, shows the uncovered P1 part (as shown in the photography of [Figure 3](#)). Below: a partial E area view (in polarized light) of the triangle, showing the P2 and P3 (encircled) particles. Numbers 5 and 22 indicate the e5 and e22 (the h1 and h2 red blood cells particles groups, respectively) particles. Number 1 indicates the e1 particle (f particle of the above [Figure 6](#) photography); the m letters indicate the various masks particles seen in this partial E area view.

tography (that of the upper [Figure 6](#) photography). As optical photographs of the triangle were taken about one year before to those taken in scanning electron microscopy, we conclude that the P2 particle was not well fixed on the surface of the sticky-tape of the triangle; it partially separates from the substrate and displaces its relative position during this time interval. Probably, the P2 particle represents in fact some form of contaminating SD material.

4. Discussion

We have found three skin debris (SD)—designated as P1, P2 and P3—at the surface of a sticky-tape triangle sampled on the Face of the Turin Shroud (TS). These SD are similar, both in ultrastructure and elementary composition, to that of one SD sampled on the face of a living man. Structurally these three SD, that have some thickness, are constituted of several layers (illustrated in Prost-Squarcioni *et al.*, 2005) and they look like desquamated skin fragments. The rough surface of P1 is similar to that of jointed corneocytes (*stratum corneum*) of the epiderm superficial part; the finely spinned surface of P3 is similar to that of jointed keratinocytes (*stratum spinosum*) of the epiderm lower part (Breathnach, 1975). Chemically they are rich in organic matter, with a marked peak of sulphur that corresponds to keratin; the P2 surface is completely covered by calcium carbonate, that hitches to see its surface ultrastructure.

Table 1 summarizes the main characteristics (concerning elementary analysis) of the three SD P1, P2 and P3. Clays are more abundant on the P1 surface. Probably because of the relatively greater P3 size compared to the other two, individualized minerals and metallic particles (accumulated here since time) are deposited on its surface.

A possibility remains that the three skin debris observed could be those of rabbit skin, a sort of glue commonly used in the painting process in some portraits. **Figure 14** shows a SEM photography of particles contained in a commercial rabbit skin glue. Rabbit skin debris are voluminous SD, with an important sickness (that

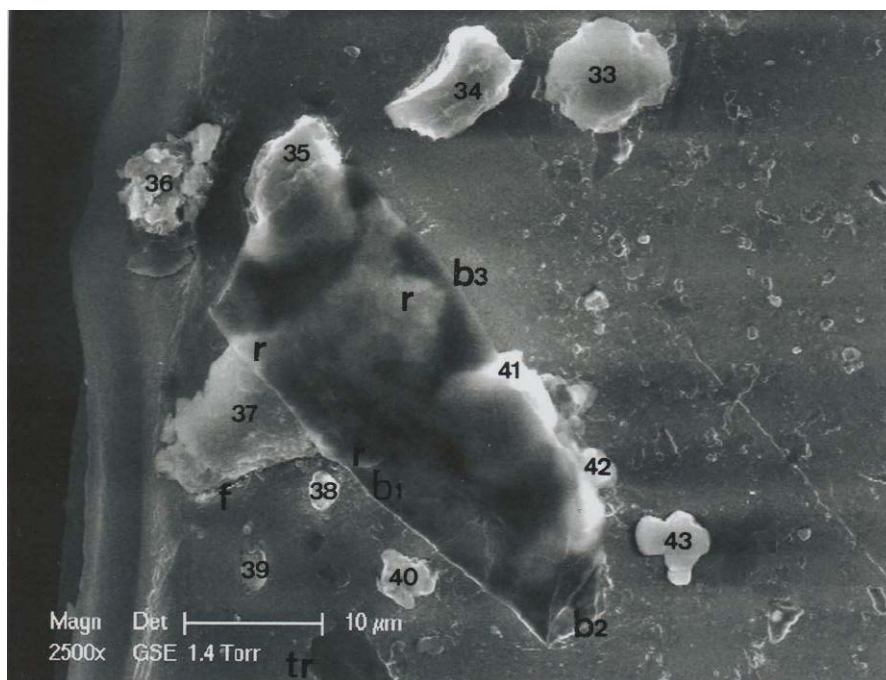


Figure 13. SEM photography (2500×) of some part of the A area of the triangle showing a (a33 to a43) particles. Number 37 indicates the a37 uncovered part of P1, and the three r the covered (by the PVC plastic) P1 part (b1, b2 and b3 show the three PVC plastic borders). Number 38 indicates the a38 particle (f: a crack in the sticky-tape, below the inferior a37 border; tr: a hole in the sticky tape).

Table 1. Main chemical characterizations of the skin debris.

Skin debris Numbers	Skin elements				Mineral overload		Mineral and metallic particles at the surface
	Organic matter	Sulphur	Chlorine	Sodium	Clays	Calcium carbonate	
P1	+	+	+	+	+++	+	No
P2	+	+	+	?	++	+++	No
P3	+	+	+	+	+	+	Yes

Footnote: + : moderate level; ++: constant level; +++: elevated level.

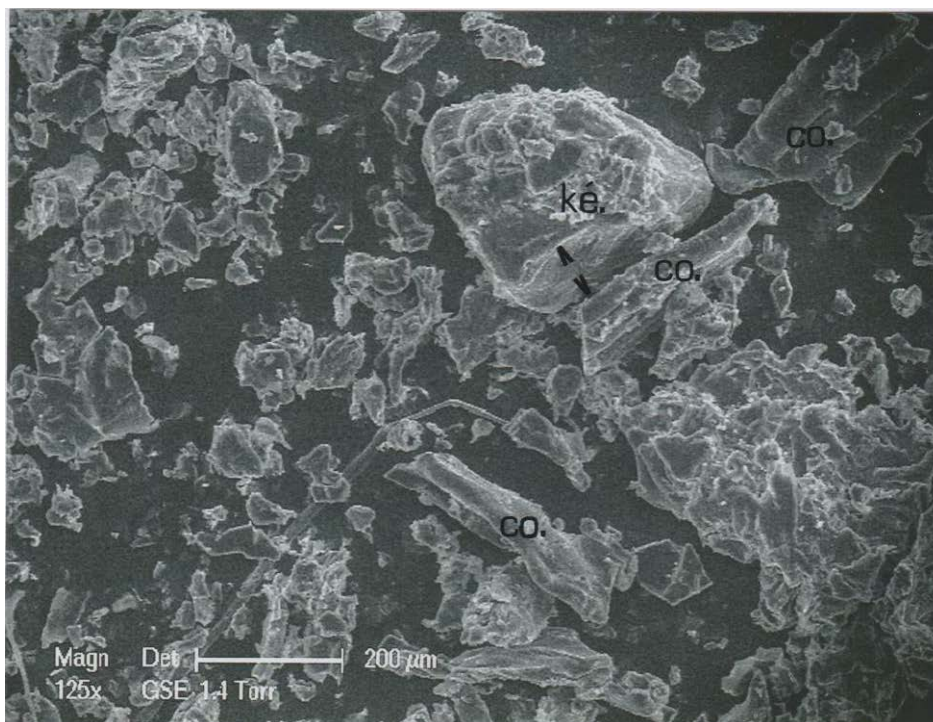


Figure 14. SEM photography (125×) of a rabbit skin glue: ké. shows a skin debris fragment of rabbit skin, and the three co. adjacents to the skin fragment are packs of collagen micro-filaments. Arrow points limit the thickness of the ké. skin fragment.

means that both epiderm and derm layers are present). Some packs of collagen micro-filaments (not found on the triangle surface) surround the rabbit skin debris (**Figure 15**) shows the peaks corresponding to organic matter and the keratin (the elevated chlorine peak corresponds mainly to salt involved in the conservative process of the skin).

Proof of the human nature of the P3 skin debris is given by the observation of the two red blood cells groups neighbouring this SD : the h1 (e5 particle) group—the hematy group h16-18 (**Lucotte, 2015c**)—and the h2 (e22 particle) group—the hematy group 19-20 (**Lucotte, 2015c**)—shown in **Figure 9**. The e5 particle adheres to (is part of) the P3 skin debris; as the human type of the red blood cells h16 - 18—like other red blood cells observed on the triangle surface (**Lucotte, 2015c**)—was proved, we infer the human nature of the P3 skin debris also. The whole of the P3 SD plus the h1 group of hematies constitutes rests of some part of a human bleeding skin.

The P1 skin debris is probably a human corneous fragment exfoliated from a finger top (where epiderm is thicker). The important calcium carbonate deposit that covers the whole P2 skin debris renders it unsuitable for further analysis.

Table 2 summarizes the five successive histological layers (Prost-Squarcioni *et al.*, 2005) of the human epiderm, from the exterior to the dermis. Skin debris P1 and P2 are constituted of the superficial layer of the cornified corneocytes only. For the SD P3—which is thicker—all the epidermal layers are conserved, because we observe on the surface (**Figure 11**) micro-spines characteristics of the *stratum spinosum* of keratinocytes; examination of the composition of the organic matter (**Figure 10**) deposited on almost all of the basal surface that there is also here some dermis micro-fragments.

Corneocytes are death-cells, without nucleus and DNA. Skin debris P3, composed of epiderm and derm layers attached, provide us an unique material to study by molecular genetics techniques the genomic components of the corresponding individual. Our current study on P3 concerns genomic DNA extractions from this peculiar skin debris.

5. Conclusion

We have found three skin debris (P1, P2 and P3) on the surface of a sticky-tape joined to the Face area of the

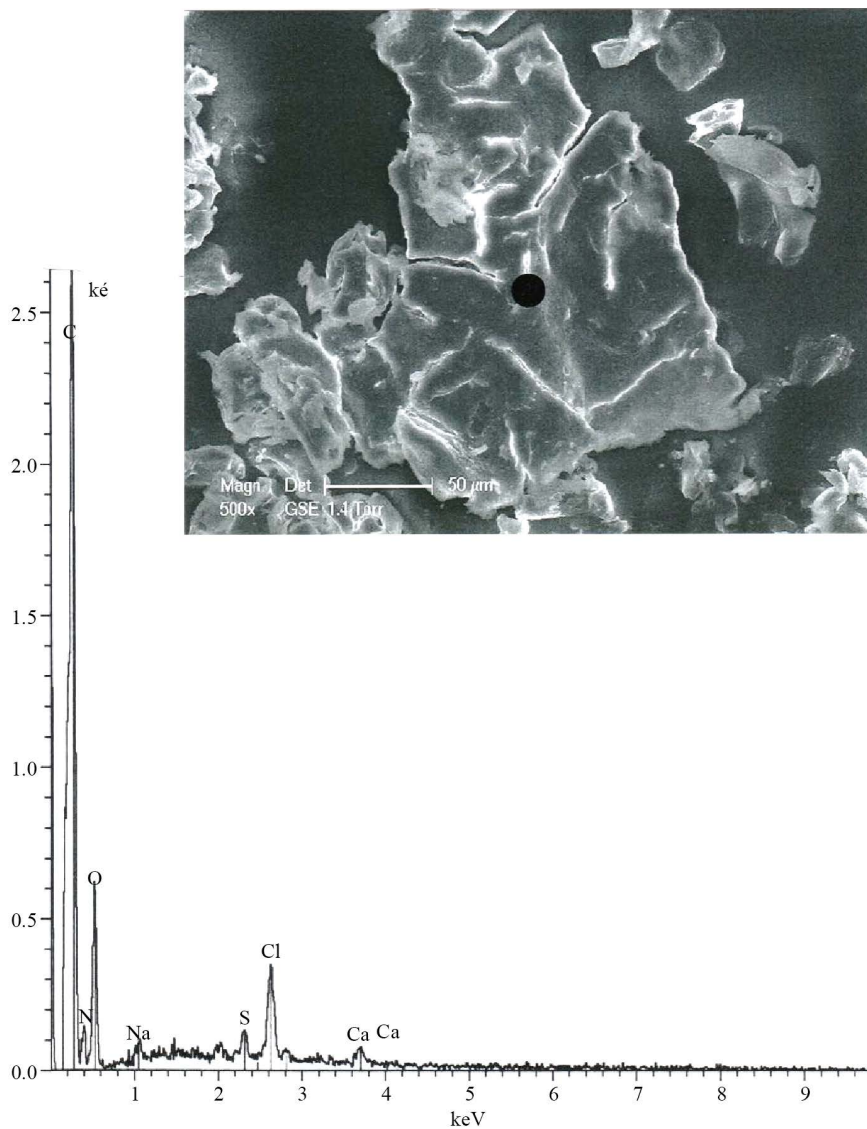


Figure 15. Above: SEM photography (500×) of a group of rabbit skin debris. Below: the corresponding spectrum (taken at the black point indicated on the photography).

Table 2. The successive layers (exterior to interior) of the epidermis.

Layers	Aspects	Cells
<i>Stratum corneum</i>	Cornified	Corneocytes
<i>Stratum lucidum</i>	White	White corneocytes
<i>Stratum granulosum</i>	Granular	Flated keratinocytes, with grains
<i>Stratum spinosum</i>	Spinous	Polygonal keratinocytes, with spines
<i>Stratum germinativum</i>	Basal	Cylindric cells

Turin Shroud. The largest one, P3, is the only one that comprises both epiderm and some part of derm layers. So, it is an excellent target tissue candidate to explore the DNA of the individual who exfoliated his skin debris on the Shroud.

Acknowledgements

We thank T. Derouin (Phanerogamy Department of the Natural History Museum of Paris) for allowing us to use his photomicroscope, and T. Thomasset (Analysis of a Physico-Chemistry Service of the UTC of Compiègne) for his precious help in SEM-EDX analysis.

References

- Burnett, B. R. (1995). Scanning Electron Microscopy/Energy Dispersive X-Ray Analysis of Gunshot Residue Associated with Clothing. *Proceedings of the American Academy of Forensic Sciences*, 1, 85. <http://dx.doi.org/10.1111/1523-1747.ep12598018>
- Breathnach, A. S. (1975). Aspects of Epidermal Ultrastructure. *Journal of Investigative Dermatology*, 65, 2-15. <http://dx.doi.org/10.1520/JFS13234J>
- DeGaetano, D., Siegel, J. A., & Klomparens, K. L. (1992). A Comparison of three Techniques Developed for Sampling and Analysis of Gunshot Residue by Scanning Electron Microscopy/Energy Dispersive X-Ray Analysis (SEM-EDX). *Journal of Forensic Sciences*, 37, 281-300.
- Lucotte, G. (2012). Optical and Chemical Characteristics of the Mineral Particles Found on the Face of the Turin Shroud. *Scientific Research and Essays*, 7, 2545-2553.
- Lucotte, G. (2015a). Exploration of the Face of the Turin Shroud. Linen Fibers Studied by SEM Analysis. *International Journal of Latest Research in Science and Technology*, 4, 78-83.
- Lucotte, G. (2015b). Exploration of the Face of the Turin Shroud. Pollens Studied by SEM Analysis. *Archaeological Discovery*, 3, 158-178. <http://dx.doi.org/10.4236/ad.2015.34014>
- Lucotte, G. (2015c). Red Blood Cells on the Turin Shroud. *Jacobs Journal of Hematology*, 2, 024.
- Marion, A., & Lucotte, G. (2006). *The Turin Shroud and Argenteuil Tunic*. Paris: Presses de la Renaissance.
- Prost-Squarcioni, C., Heller, M., & Fraitag, S. (2005). Histology and Histophysiology of the Skin and Its Annexes. *Annales de Dermatologie et Vénérologie*, 132, 835-848.
- Riggi di Numana, G. (1988). *Sindone Report 1978/1987*. Milano: Ed. 3M.
- Varetto, L. (1990). The Use of Plasma Ashing on Samples for Detection of Gunshot Residues with Scanning Electron Microscopy and Energy Dispersive X-Ray Analysis. *Journal of Forensic Sciences*, 35, 964-970. <http://dx.doi.org/10.1520/JFS12912J>